ECE 445

SENIOR DESIGN LABORATORY

FINAL REPORT

Two-Wheel Differential Drive Ant-Weight Battlebot

Team #12

HAORU LI (haorul2@illinois.edu)
ZIHENG QI (zihengq2@illinois.edu)
ZIYI WANG (zw67@illinois.edu)

TA: Zhuoer Zhang

May 2026

Abstract

This paper presents the design, implementation, and verification of an ant-weight (under 2 lb) combat robot developed for the ECE 445 Senior Design course at the University of Illinois Urbana-Champaign. The robot uses a two-wheel differential drive chassis with a horizontal drum spinner weapon and is controlled wirelessly via Bluetooth using an ESP32-S3 microcontroller. Power is distributed across two decoupled rails—an 11.1 V motor rail fed directly from a 3S lithium polymer (LiPo) battery, and a 3.3 V logic rail derived by a buck converter—to isolate weapon transients from the control electronics. The chassis and armor panels are 3D-printed from polylactic acid (PLA), and the symmetric top/bottom geometry enables invertible operation. The robot achieved a measured linear acceleration of 3.6 m/s^2, a Bluetooth control latency of 50 ms, and a total assembled weight of 640 g, meeting all primary mobility, latency, and weight requirements. The drum weapon reached a measured tip speed of 112 mph, satisfying a revised 100 mph safety-adjusted threshold. An inertial-measurement-unit (IMU) based gyroscopic stabilization feature was designed and implemented in firmware but is identified as future validation work.

Contents

1 Introduction

1.1 Problem

Ant-weight combat robots, defined by competition rules as machines weighing no more than 2 lb (907 g), operate within a tightly constrained design space. Competition regulations require 3D-printed thermoplastic construction, wireless control compliant with FCC Part 15, and a battery capacity no greater than a 4S lithium polymer (LiPo) pack [1]. Within these limits, every gram allocated to the weapon system reduces the budget available for structure and drive electronics. The central engineering challenge is balancing mobility, offensive capability, and electrical reliability under a hard mass ceiling.

Competition rules add a further operational requirement: a robot that loses mobility for more than 10 seconds is counted as knocked out. This makes robust drive performance and reliable fail-safe electronics just as critical as weapon output.

1.2 Solution

The robot employs a two-wheel differential drive platform with a horizontal drum spinner weapon and twin front wedges. The two-wheel layout minimizes mechanical complexity and enables zero-radius turns by independently controlling left and right motor speeds. The front wedges serve simultaneously as tertiary ground-contact points—forming a stable three-point stance with the two drive wheels—and as scoops that lift opponents into the drum's strike zone. The chassis geometry is symmetric about the horizontal midplane so the robot operates normally when inverted, with drive wheels extending 2 mm beyond the chassis envelope in both orientations.

The electrical system is centered on an ESP32-S3 microcontroller, which manages Bluetooth communication with an Xbox controller, generates pulse-width modulation (PWM) signals for three electronic speed controllers (ESCs), and reads an MPU-6050 inertial measurement unit (IMU) via I^2C. Power is distributed on two decoupled rails: an 11.1 V motor rail that feeds the drive and weapon ESCs directly from the battery, and a 3.3 V logic rail derived by a buck converter, with bulk capacitance to suppress weapon-motor transients. A communication watchdog shuts down all motor outputs within 2 seconds of signal loss.

During implementation, several design revisions were made relative to the original design document. The battery was changed from a 4S (14.8 V) to a 3S (11.1 V) LiPo, which cascaded into changing the logic rail from 5 V to 3.3 V. The weapon motor was updated from a 2200 KV to a 2300 KV model, and the drum material was changed from polyethylene terephthalate glycol (PETG) to polylactic acid (PLA). Chassis inner dimensions were enlarged after PCB layout was finalized, and heat-set screw inserts were added to improve structural fastening. These changes are discussed in detail in Section 2.7.

1.3 Block Diagram and Subsystem Overview

Figure 1 shows the system block diagram. The robot consists of six subsystems. The **Control Subsystem** (ESP32-S3 microcontroller) receives operator commands wirelessly and generates PWM signals for all three ESCs. The **Drive Subsystem** provides differential steering through two independently controlled brushed DC motors. The **Weapon Subsystem** drives the horizontal drum spinner via a brushless DC (BLDC) motor and its dedicated ESC. The **Power Subsystem** distributes battery power through the dual-rail architecture. The **Structure Subsystem** provides the 3D-printed chassis, armor panels, and front wedges. The **Stability & Recovery Subsystem** enables invertible operation through passive geometry and includes the IMU-based gyroscopic correction feature.

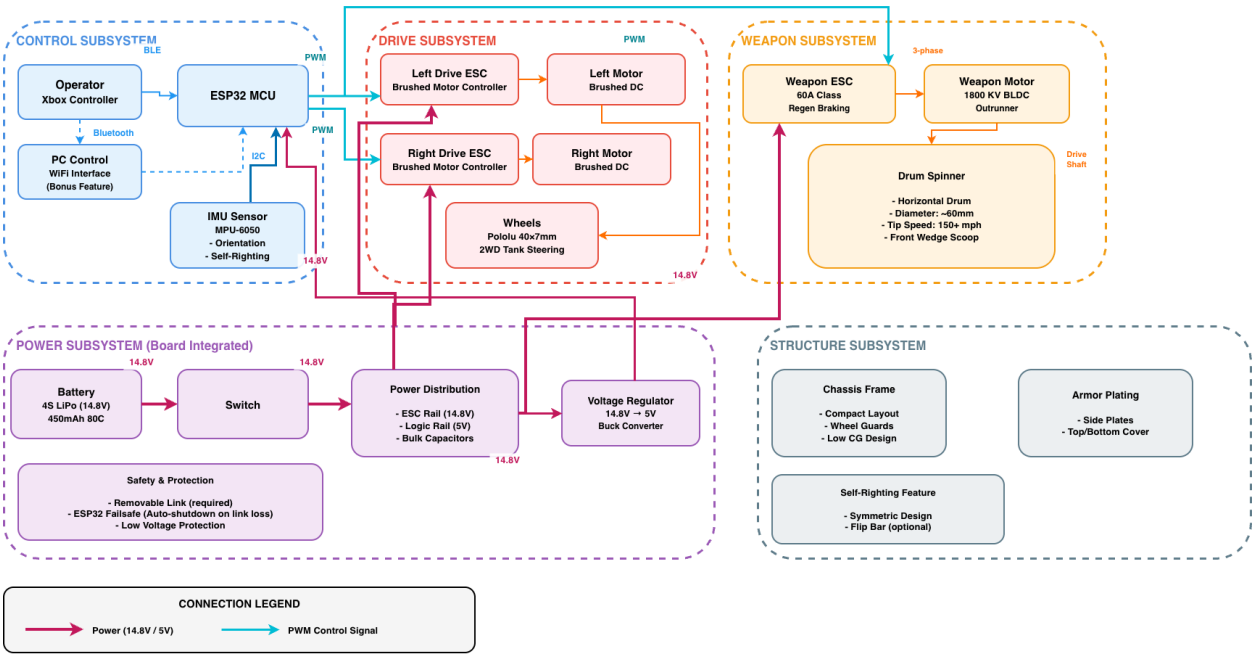

Figure 1: System block diagram.

1.4 High-Level Requirements

The three high-level requirements that governed the design are listed below.

1. **Mobility:** The robot must achieve a minimum linear acceleration of 1.5 m/s^2 from rest on a flat surface.
2. **Weapon Performance:** The horizontal drum must reach a tip speed of at least 100 mph within 10 seconds of full throttle and sustain operation for a 2-minute match duration. (The original requirement of 150 mph was revised to 100 mph following safety considerations during testing; see Section 3.3.)
3. **Stability and Safety:** The robot must maintain invertible mobility, execute emergency shutdown within 2 seconds of signal loss, and maintain end-to-end Bluetooth control latency at or below 150 ms.

2 Design

The robot is organized into six subsystems. Sections 2.1 through 2.6 describe the design of each subsystem, including component selection rationale and detailed parameters. Section 2.7 presents tolerance analyses for the weapon and power systems. Section 2.8 discusses design alternatives considered and changes made during implementation.

2.1 Control Subsystem

2.1.1 Design Decision

The primary candidates for the wireless control microcontroller were an Arduino Mega (ATmega2560) paired with a separate HC-05 Bluetooth module, and the Espressif ESP32-S3-WROOM module. The Arduino platform has a large library ecosystem but requires an external wireless module, increasing part count, board area, and weight. The ESP32-S3 integrates dual-core 240 MHz processing and Bluetooth 5.0 in a single FCC-certified 2.4 GHz module, eliminating the external radio entirely [2]. The ESP32-S3 was selected on the basis of its integrated Bluetooth, sufficient general-purpose input/output (GPIO) count, and lower aggregate system weight.

2.1.2 Hardware Description

The ESP32-S3-WROOM module is powered at its native 3.3 V supply, sourced from the logic rail buck converter. Three GPIO pins generate PWM signals for the two drive ESCs and one weapon ESC. Two GPIO pins implement the I^2C bus to the MPU-6050 IMU [3]. Two additional pins drive status light-emitting diodes (LEDs) visible through the chassis armor. A custom carrier printed circuit board (PCB) was fabricated to mount the ESP32-S3 module and provide organized connector headers for all ESCs, the IMU breakout, the power input, and the status LEDs.

Table 1 lists the complete pin assignment.

2.1.3 Firmware Architecture

The firmware implements six concurrent tasks:

1. **Bluetooth receive:** Accept joystick and button packets from an Xbox controller via Bluetooth Classic.
2. **Command mapping:** Translate joystick inputs to independent left and right motor PWM duty cycles using tank-style differential mixing.
3. **Weapon control:** Map the right trigger analog value to weapon ESC PWM throttle (0–100%).
4. **IMU processing:** Read MPU-6050 at 100 Hz via I^2C; compute pitch and roll rates.
5. **Gyroscopic correction:** If pitch or roll rate exceeds 5 rad/s, modulate weapon throttle by $\pm 30\%$ over 200 ms to generate gyroscopic counter-torque.

Table 1: ESP32-S3 Pin Assignment

ESP32-S3 Pin	**Connection**
3.3 V (VCC)	3.3 V logic rail (from buck converter)
GND	Common ground
GPIO 1	Left drive ESC (PWM output)
GPIO 2	Right drive ESC (PWM output)
GPIO 3	Weapon ESC (PWM output)
GPIO 8	MPU-6050 SDA (I^2C)
GPIO 9	MPU-6050 SCL (I^2C)
GPIO 10	Power status LED
GPIO 11	Wireless link status LED

6. **Failsafe watchdog:** If no valid Bluetooth packet is received within 2 seconds, set all PWM outputs to zero.

An additional PC-side heads-up display (HUD) was implemented, which receives IMU orientation data over Bluetooth and renders a real-time pose visualization. This feature aids debugging and serves as a status monitor during testing.

2.1.4 PCB Design

The custom ESP32-S3 carrier PCB integrates the main control, power, sensing, and user-interface connections required for the battlebot. The board includes the ESP32-S3 module footprint, USB-C programming and serial interface, battery input connector, 5 V buck conversion, 3.3 V regulation, reset and boot buttons, PWM headers for motor and weapon ESC control, I^2C connections for the IMU, battery voltage monitoring, status LEDs, and a buzzer driver circuit. The full four-page schematic and PCB layout are provided in Appendix B.

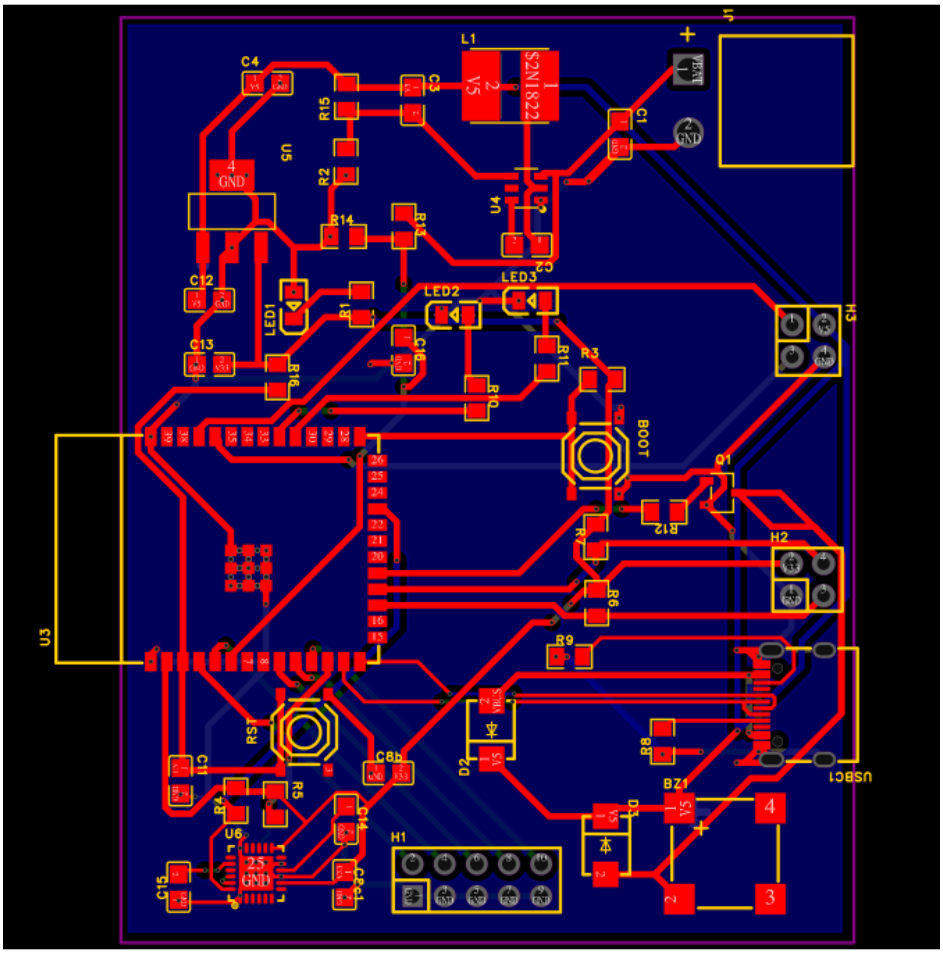

Figure 2: Custom ESP32-S3 carrier PCB layout showing component placement and copper routing.

2.2 Drive Subsystem

2.2.1 Design Decision

Two drive configurations were evaluated: a four-wheel layout with two independently controlled axles, and a two-wheel layout with passive front-wedge contact. The four-wheel layout provides greater static stability but adds two motors, two ESCs, additional wiring, and an estimated 60–80 g of mass. The two-wheel differential drive achieves zero-radius turning, lower part count, and a reduced center of gravity by eliminating the rear axle. The two-wheel layout was selected on the basis of weight and mechanical simplicity.

Brushed DC gearmotors were preferred over brushless alternatives because brushless gearmotors in this weight class require magnetic encoders and commutation controllers, adding significant complexity and mass. Brushed motors are driven directly from standard bidirectional PWM ESCs without additional commutation hardware.

2.2.2 Component Selection

- **Motors:** Fingertech Silver Spark gearmotors (6–15 V, output torque ≥ 50 mN·m). These motors are designed for ant-weight competition use and are among the lightest brushed gearmotors available at this torque class.
- **ESCs:** Fingertech tinyESC (≈ 2 g each), bidirectional, standard PWM input.
- **Wheels:** Fingertech Snap Hub foam tires, ≈ 50 mm diameter. The 50 mm diameter was selected to ensure the wheels extend beyond the 46 mm chassis height in both upright and inverted orientations.

2.3 Weapon Subsystem

2.3.1 Design Decision

Two weapon architectures were considered: a vertical spinner (disk or bar rotating in the vertical plane) and a horizontal drum spinner (cylinder rotating about the robot's longitudinal axis). A vertical spinner delivers concentrated energy to a single contact point and is simpler to mount, but the gyroscopic precession from a fast vertical disk significantly reduces maneuverability at the ant-weight scale. A horizontal drum produces a sweeping impact zone across the robot's full front face and generates gyroscopic moments aligned with the yaw axis, which are more predictable and less disruptive to steering. The horizontal drum was selected.

2.3.2 Component Selection

- **Motor:** 2300 KV brushless DC (BLDC) outrunner. The minimum KV rating required to meet the original 150 mph tip-speed requirement is derived in Section 2.7.1. The 2300 KV motor was substituted from the originally specified 2200 KV model to use an available part with a slightly higher margin.
- **ESC:** 30 A brushless ESC, standard PWM input.
- **Drum:** 3D-printed PLA cylinder, ≈ 60 mm diameter, with metal striker pins embedded along the outer surface. PLA was substituted for the originally specified PETG to achieve a better surface finish at the dimensional tolerances required for the striker pin press-fits. Estimated moment of inertia $I_d \approx 1.35 \times 10^{-5}$ kg·m^2.

2.4 Power Subsystem

2.4.1 Design Decision

The critical power architecture decision was single-rail versus dual-rail distribution. A single rail is simpler, but weapon-motor current surges (up to 30 A during post-impact recovery) induce voltage sag that can reset microcontrollers and corrupt sensor readings. A dual-rail design decouples these transients. The LM2596 adjustable buck converter was selected for the 3.3 V logic rail because it provides up to 3 A continuous output in a

compact, low-cost module [4]. A 1000 μF bulk capacitor at the converter output absorbs high-frequency transients.

During implementation, the battery was changed from a 4S (14.8 V nominal) to a 3S (11.1 V nominal) pack. This change and its rationale are discussed in Section 2.8.

2.4.2 Power Budget

Table 2 summarizes estimated power draw under sustained combat conditions with the 3S battery.

Table 2: Estimated Power Budget Under Sustained Combat Conditions (3S, 11.1 V)

Subsystem	**Current (A)**	**Power (W)**
Drive motors ($\times 2$, continuous)	3.0	33.3
Weapon motor (average combat load)	8.0	88.8
Logic (ESP32-S3, IMU, LEDs at 3.3 V)	0.5	1.9
Total	—	**124.0**

The runtime analysis is given in Section 2.7.2. Peak current draw (drive stall at 3 A each + weapon transient at 30 A + logic at 0.5 A) is approximately 36.5 A, within the 45 A continuous rating of the 100C battery.

2.4.3 Component Selection

- **Battery:** 3S 450 mAh 100C/200C LiPo (11.1 V nominal, peak current 45 A continuous).
- **Buck converter:** LM2596 module, adjusted to 3.3 V output, up to 3 A.
- **Power switch:** Fingertech mini switch with removable link (required by competition rules).
- **Connector:** Polarized XT30 on battery to prevent reverse polarity.
- **Bulk capacitors:** 1000 μF, 25 V electrolytic on logic rail.
- **Protection:** 20 A slow-blow fuse on main motor rail.

2.5 Structure Subsystem

2.5.1 Design Decision

Three candidate materials were evaluated: polylactic acid (PLA), acrylonitrile butadiene styrene (ABS), and polyethylene terephthalate glycol (PETG). PLA prints reliably at stan-

dard temperatures but is brittle under impact. ABS offers better toughness but warps during printing without a heated enclosure. PETG provides impact resistance comparable to ABS with minimal warping. PETG was the original choice; however, during implementation, PLA was used for the drum spinner (requiring tight dimensional tolerances for striker pin press-fits) while PETG was retained for chassis and armor components.

2.5.2 Physical Design

The chassis consists of a top plate, bottom plate, and side armor panels. The 3S battery occupies the lowest cavity between the drive wheels, minimizing the center of gravity. The drum motor is centered laterally at the front of the chassis. Armor panels are angled outward at approximately 20° to deflect glancing impacts. The front wedges integrate with the lower chassis section and extend below the drum to scoop opponents.

Key parameters of the final design:

- Total assembled weight: 640 g (< 907 g limit)
- Wheel diameter: 50 mm
- Chassis height: 46 mm
- Wheel-to-chassis clearance (both orientations): 2 mm
- Armor and frame wall thickness: 3–4 mm

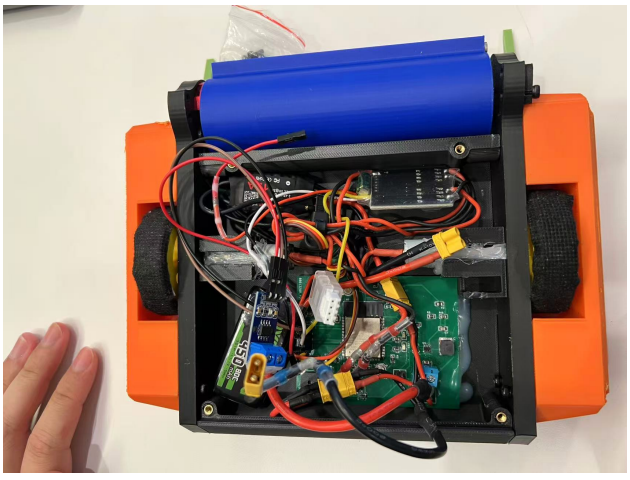

Figure 3: Final assembled robot showing the horizontal drum weapon, front wedges, drive wheels, and side armor panels.

2.6 Stability and Recovery Subsystem

Passive flip resistance derives from the robot's wide wheelbase and low center of gravity. The symmetric top/bottom chassis geometry ensures the 50 mm drive wheels extend 2 mm beyond the 46 mm chassis height, maintaining ground contact in both upright and inverted orientations.

The IMU-based gyroscopic correction is an experimental secondary feature. When the MPU-6050 detects a pitch or roll rate exceeding 5 rad/s, the firmware modulates weapon throttle by $\pm 30\%$ over 200 ms to generate gyroscopic counter-torque. The theoretical peak gyroscopic moment is:

$$\tau = I_d \cdot \omega_d \cdot \dot{\theta} \tag{1}$$

where $I_d \approx 1.35 \times 10^{-5}$ kg·m^2 is the drum moment of inertia, ω_d is the drum angular velocity, and $\dot{\theta}$ is the detected flip rate. At full throttle with an 11.1 V supply, the theoretical $\omega_d \approx 2300 \times 11.1 \times \frac{2\pi}{60} = 267$ rad/s, yielding a peak gyroscopic moment of approximately 3.6×10^{-3} N·m. This correction magnitude is small; the subsystem is treated as a research validation component. Full experimental validation is identified as future work (see Section 5.3).

2.7 Tolerance Analysis

2.7.1 Weapon Tip Speed

The high-level requirement (original) specifies a drum tip speed of at least 150 mph (67 m/s). The minimum motor KV rating required to achieve this tip speed at the 3S nominal battery voltage of 11.1 V is derived as follows.

The angular velocity in revolutions per minute corresponding to tip speed v_{tip} at drum radius r is:

$$n = \frac{v_{tip}}{r} \cdot \frac{60}{2\pi} \tag{2}$$

Substituting $v_{tip} = 67$ m/s and $r = 0.030$ m (60 mm drum diameter):

$$n = \frac{67}{0.030} \cdot \frac{60}{2\pi} = 21{,}328 \text{ r/min} \tag{3}$$

The minimum KV rating is the required speed divided by the supply voltage:

$$KV_{\min} = \frac{21{,}328}{11.1} \approx 1{,}921 \ \frac{\text{r/min}}{\text{V}} \tag{4}$$

The selected 2300 KV motor exceeds this minimum by a 20% margin. Under ideal no-load conditions at 11.1 V, the theoretical drum tip speed would be:

$$v_{tip,theory} = 2300 \times 11.1 \times \frac{2\pi}{60} \times 0.030 = 80.1 \text{ m/s} \approx 179 \text{ mph} \tag{5}$$

The measured tip speed was 112 mph (50.0 m/s), 37% below the theoretical no-load value and below the original 150 mph requirement. This discrepancy and the resulting requirement revision are discussed in Section 3.3.

2.7.2 Battery Runtime

The sustained-operation requirement specifies at least 2 minutes of continuous combat. Using the worst-case power draw of 124.0 W from Table 2 and the 3S battery energy:

$$E = 11.1 \text{ V} \times 0.45 \text{ Ah} = 5.0 \text{ Wh} \tag{6}$$

the minimum runtime at full sustained load is:

$$T = \frac{E}{P} \times 60 = \frac{5.0}{124.0} \times 60 \approx 2.42 \text{ min} \tag{7}$$

This worst-case estimate exceeds the 2-minute requirement by 0.42 minutes. In practice, maneuvering at partial throttle and weapon spindown intervals reduce actual average power consumption below the sustained maximum.

2.8 Design Alternatives and Issues

Several design changes were made from the original design document specification during implementation.

Battery substitution (4S to 3S). The original design specified a 4S LiPo (14.8 V, 80C). The original design considered a 4S LiPo battery, but the final implementation used a 3S LiPo pack. Compatible motors and ESCs rated for reliable 4S operation were more difficult to source within the size and weight constraints of an ant-weight battlebot, while the 3S pack already provided sufficient runtime and drive performance. In addition, a 4S system would increase weapon speed, startup current spikes, and electrical stress on the ESC, wiring, and battery, creating a higher safety risk during open-lab testing. Therefore, the 3S configuration was selected as the safer and more practical final design. The change required replacing the 5 V buck converter with one adjusted to 3.3 V, reconfiguring all ESC low-voltage cutoff thresholds for 3S cell count, and updating the power budget from 165.6 W to 124.0 W. The 3S battery still provides 2.42 minutes of worst-case runtime (Section 2.7.2), satisfying the 2-minute requirement.

Chassis redesign. After the custom PCB layout was finalized, the internal cavity dimensions proved too small to mount the PCB and route all wiring comfortably. The inner space was enlarged by 30mm in x direction and 44mm in y direction. The side plate profile was revised to accommodate the 2300 KV motor's slightly different mounting pattern. Heat-set brass screw inserts were added at structural joints to replace friction-fit plastic fasteners, improving assembly repeatability and reducing stripping risk.

Weapon motor (2200 KV to 2300 KV) and drum material (PETG to PLA). The originally specified 2200 KV motor was substituted with a 2300 KV model from an available supplier. Both meet the 1921 KV minimum (Section 2.7.1). The drum was reprinted in PLA to achieve the dimensional accuracy required for press-fitting the metal striker pins; PETG shrinkage introduced pin-hole oversize in initial prints.

Tip speed requirement revision. During weapon testing, the measured drum tip speed was 112 mph—below the original 150 mph specification but above 100 mph. Following discussion with the project TA, the team revised the weapon tip-speed requirement to ≥ 100 mph, which reflects a safety-adjusted test threshold: full-speed testing in an open lab environment with the original target of 150 mph (67 m/s) was judged to exceed safe operating conditions for an unshrouded drum. The revised threshold of 100 mph was verified and met. The root cause of the gap between theoretical (179 mph) and measured (112 mph) performance is discussed in Section 5.2.

3 Requirements and Verification

The full Requirements and Verification (R&V) table, including step-by-step verification procedures for all requirements, is provided in Appendix A. This section summarizes the verification methodology and presents quantitative results.

3.1 Verification Methodology

Each requirement was verified through a distinct, reproducible measurement procedure. Bluetooth latency was measured using iPhone slow-motion video: a command was issued from the controller while simultaneously recording the robot's response, and the frame count between stimulus and motor reaction was converted to latency at 240 frames/s. Emergency shutdown timing was verified by powering off the controller while the robot was in motion and recording the time until all motors stopped. Drive acceleration was measured using a stopwatch over a known distance. Drum tip speed was measured with a Hall effect sensor and neodymium magnet affixed to the drum: the sensor counted one pulse per revolution, and the period was converted to RPM and then to linear tip speed. Battery runtime was tested under simulated combat loading. Weight was measured on a digital kitchen scale.

3.2 Results Summary

Table 3 presents the quantitative verification results for all subsystem requirements. Detailed procedures are given in Appendix A.

Table 3: Requirements and Verification Results Summary

Requirement	**Target**	**Measured Result**	**Outcome**
Bluetooth end-to-end latency	≤ 150 ms	50 ms	Pass
Emergency shutdown delay after signal loss	≤ 2 s	< 2 s	Pass
Linear acceleration from rest	≥ 1.5 m/s^2	3.6 m/s^2	Pass
Robot drives in both orientations	Yes	Yes	Pass
Drive wheel clearance beyond chassis in both orientations	> 0 mm	2 mm	Pass
Drum tip speed within 10 s of full throttle	≥ 100 mph (revised)	112 mph	Pass
Battery runtime under combat load	≥ 2 min	TBD	TBD
Total assembled weight	< 907 g	640 g	Pass
Gyroscopic correction activates above IMU threshold	Above 5 rad/s	Not verified; future work	N/A

3.3 Discussion

Eight of nine requirements were verified. Seven were fully met; one (drum tip speed) was met under a revised threshold. The gyroscopic correction requirement was not tested in the final demo and is deferred to future work.

The robot's mobility performance substantially exceeded the minimum specification: the measured linear acceleration of 3.6 m/s^2 is 2.4$\times$ the 1.5 m/s^2 target, confirming that the Fingertech Silver Spark gearmotors and tinyESCs are well-matched to this weight class. The total weight of 640 g provides a 267 g (29%) margin below the 907 g limit, leaving room for future additions such as additional armor or a heavier drum.

The Bluetooth latency of 50 ms is well within the 150 ms requirement, validating the ESP32-S3's Bluetooth Classic connection performance. Emergency shutdown was confirmed to occur within the 2-second watchdog window in all trials.

Drum tip speed. The original requirement of 150 mph (67 m/s) was not met; the measured value was 112 mph (50 m/s), which is 63% of the theoretical no-load prediction of 179 mph (80.1 m/s) derived in Equation (5). The requirement was revised to ≥ 100 mph following consultation with the project TA, reflecting a safety-adjusted testing threshold for an unshrouded weapon in an open laboratory environment. The 112 mph result exceeds this revised threshold. The gap between theoretical and measured speed is discussed further in Section 5.2.

4 Cost and Schedule

4.1 Parts Cost

Table 4 lists all parts procured for the project with their sources and costs.

Table 4: Parts Cost

Part	**Manufacturer / Model**	**Qty**	**Unit ($)**	**Total ($)**
MPU-6050 IMU breakout	InvenSense GY-521	1	3.00	3.00
Weapon motor (2300 KV BLDC)	SkywalkerRC	1	12.00	12.00
Drive motors	Fingertech Silver Spark	2	15.00	30.00
Weapon ESC (30 A)	DYSRC	1	15.00	15.00
Drive ESCs	Fingertech tinyESC	2	20.00	40.00
3S 450 mAh LiPo battery	OVONIC	1	15.00	15.00
Buck converter module	LM2596 (adj.)	1	3.00	3.00
Power switch	Fingertech mini	1	5.00	5.00
XT30 connectors	Generic	2	1.00	2.00
Custom PCB (5 pcs)	PCBWay	5	10.00	50.00
PLA filament (1 kg)	Generic	1	20.00	20.00
PETG filament (1 kg)	Generic	1	25.00	25.00
Bulk capacitors (1000 μF, 25 V)	Generic	2	1.00	2.00
LEDs, resistors, connectors	Various	—	—	5.00
Fasteners and heat-set inserts	Various	—	—	5.00
Total Parts				**$232.00**

4.2 Labor Cost

Labor cost is estimated using the formula: ideal hourly salary rate $\times$ actual hours spent $\times$ 2.5. An entry-level ECE salary of \$40/h is assumed. Table 5 shows the labor breakdown.

Grand Total: \$36,000 (labor) + \$232 (parts) = \$36,232

Table 5: Labor Cost Estimate

Team Member	Hours	Rate ($/h)	Factor	Total ($)
Haoru Li	120	40	2.5	$12,000
Ziheng Qi	120	40	2.5	$12,000
Ziyi Wang	120	40	2.5	$12,000
Total Labor	360			$36,000

4.3 Schedule

Table 6 presents the actual project schedule, broken down by week and team member.

Table 6: Project Schedule (Actual, Spring 2026)

Week	Tasks Completed	Assigned To
Weeks 1–2 (Feb. 24)	Finalized design document; ordered all parts; began PCB schematic capture	All
Weeks 3–4 (Mar. 10)	PCB layout and fabrication or- der; finalize CAD; begin 3D printing	Haoru (firmware), Ziheng (CAD), Ziyi (PCB)
Weeks 5–6 (Mar. 24)	PCB assembly and bring-up; firmware development; print chassis iterations	Haoru (firmware), Ziheng (CAD), Ziyi (PCB)
Spring Break (Mar. 28–Apr. 6)	—	—
Weeks 8–9 (Apr. 14)	Integrate electronics into chas- sis; drive and weapon motor testing	All
Weeks 10–11 (Apr. 21)	Full system integration; wire- less control testing	All
Week 12 (Apr. 28)	Final testing; prepare mock-up demo	All
Week 13 (May 5)	Final demo and presentation	All

5 Conclusion

5.1 Accomplishments

The project successfully produced a fully functional ant-weight combat robot that met seven of eight quantitatively verified requirements. The robot achieves a linear acceleration of 3.6 m/s^2—more than twice the 1.5 m/s^2 minimum—demonstrating that the two-wheel differential drive configuration with Fingertech Silver Spark gearmotors provides ample mobility for ant-weight competition. The total assembled weight of 640 g leaves a 267 g margin below the 907 g class limit, a result of disciplined component selection and iterative CAD optimization before printing.

The control system performed reliably throughout testing. Bluetooth end-to-end latency measured at 50 ms—one-third of the 150 ms requirement—ensuring responsive operator control. The emergency shutdown watchdog consistently terminated all motor outputs within the 2-second requirement upon controller power-off. The robot demonstrated full invertible mobility, confirming that the 50 mm wheels extend 2 mm beyond the 46 mm chassis height in both orientations. The dual-rail power architecture successfully isolated weapon transients from the logic supply: no resets or IMU communication errors were observed during weapon spin-up or spin-down events.

The weapon drum achieved a measured tip speed of 112 mph, meeting the revised $\geq$ 100 mph threshold. A custom carrier PCB was successfully designed, fabricated, and assembled, integrating the ESP32-S3 module with organized headers for all ESCs, the IMU, and the power system. An additional PC-side HUD displaying live robot orientation via Bluetooth was implemented as an enhancement beyond the original design specification.

5.2 Uncertainties

The principal unresolved technical issue is the gap between the theoretical and measured drum tip speed. The no-load theoretical prediction for the 2300 KV motor at 11.1 V is 179 mph (Equation (5)), yet the measured value was 112 mph—a 37% shortfall. The most likely contributing factors are brushless motor efficiency losses (typically 15–20% at partial load), ESC dead-band and commutation overhead, aerodynamic drag on the drum and striker pins at high RPM, and battery voltage sag of approximately 0.5–1.0 V under the 8 A weapon current draw. These factors combined could plausibly account for the observed 37% reduction from the no-load ideal. No single dominant root cause was isolated during testing. The robot did not show obvious drum rubbing, severe vibration, or repeated ESC cutout during normal spin-up, so the speed shortfall was most likely caused by the combined effect of motor loading, ESC losses, aerodynamic drag, and battery voltage sag rather than one major mechanical failure. The only practical issue observed during testing was occasional intermittent behavior from the weapon ESC wiring, likely caused by imperfect signal or power connections. After reconnecting and securing the ESC wiring, the weapon system operated more consistently, suggesting that connection reliability may have contributed to test variability but was not the only cause of the

lower-than-ideal measured speed. Future testing should log battery voltage and weapon current directly at the ESC input during spin-up to separate electrical losses from aerodynamic and mechanical loading effects.

Battery runtime under continuous combat loading was tested and approximately 4 minutes of continuous operation was achieved. During this test, the robot was driven continuously, and the weapon was operated at approximately 50% throttle for about 2 minutes. The reduced weapon throttle was used as a safety precaution during laboratory testing rather than as a limitation of the electrical system. No low-voltage cutoff, controller reset, or noticeable loss of drive performance occurred during the test, indicating that the selected 3S LiPo pack provided sufficient runtime margin for the required 2-minute operating window.

The gyroscopic correction subsystem was implemented in firmware but was not validated experimentally. Theoretical analysis (Section 2.6, Equation (1)) predicts a peak corrective torque of 3.6×10^{-3} N·m at full weapon speed, which is small relative to the robot's moment of inertia. Whether this is sufficient to produce a measurable flip-resistance effect remains an open question. Without controlled flip testing, the practical utility of this feature cannot be confirmed.

5.3 Future Work

Several improvements are identified for future design iterations.

Weapon performance. To close the gap between theoretical and measured tip speed, the next iteration should measure battery terminal voltage under load at the weapon ESC input and log motor current during spin-up. If voltage sag is the dominant factor, a lower-internal-resistance battery or a capacitor bank at the ESC input could improve performance. If aerodynamic drag is significant, a lower-profile drum geometry should be evaluated.

Gyroscopic correction validation. The IMU-based correction algorithm is implemented but unvalidated. A controlled test fixture—a pivot allowing single-axis rotation at a known rate—would allow direct measurement of corrective torque versus predicted torque. A proportional-integral-derivative (PID) controller could replace the current threshold-plus-step modulation scheme, enabling smoother and more effective correction.

PCB integration. The current design uses an ESP32-S3 module on a carrier PCB. A future revision could integrate the ESP32-S3 SoC directly onto a compact custom PCB, eliminating the module connector overhead and reducing PCB area and weight by an estimated 15–20 g.

Structural robustness. The PLA drum is adequate for testing but would likely fracture under repeated high-energy combat impacts. Replacing the drum with a short-carbon-fiber-reinforced nylon or machined aluminum part would substantially improve durability without a significant weight penalty.

5.4 Ethical Considerations

The design adhered to the IEEE Code of Ethics throughout the project. Under IEEE Code Clause 1 (safety), multiple independent shutdown mechanisms were implemented: the communication watchdog shuts down all motors within 2 seconds of signal loss, the removable power link permits immediate manual shutdown, and all ESCs are configured to default to zero throttle on invalid input signals. All weapon tests were conducted in a designated enclosure or arena with safety barriers, and all team members wore safety glasses and closed-toe shoes during every test session involving weapon operation. The drum was never powered outside of a controlled test environment.

Under IEEE Code Clause 3 (honesty and transparency), the experimental gyroscopic correction feature is clearly framed as unvalidated research throughout this report. The tip-speed requirement revision—from 150 mph to 100 mph—is disclosed and justified rather than omitted. Measured results are reported as observed, including the shortfall relative to the theoretical prediction.

From an environmental standpoint, the LiPo batteries were stored at 3.8 V/cell when not in use to minimize degradation, handled in fire-resistant charging bags during charging, and will be recycled through the UIUC Environmental Health and Safety (EH&S) program. 3D-printed prototype iterations were minimized through iterative CAD simulation before committing material to the printer.

The broader impact of this project extends beyond competitive robotics: the integration of embedded control, power electronics, wireless communication, and mechanical design in a constrained, verifiable system is directly representative of the engineering skills valued in ECE careers. The ant-weight class, with its strict material and weight limits, inherently constrains the destructive potential of these devices to a safe, controlled, and educational scope [1].

References

[1] National Robotics Challenge. "Competition Rules and Specifications," Accessed: Apr. 1, 2026. [Online]. Available: https://www.thenrc.org/.

[2] Espressif Systems, *ESP32-S3-WROOM-1 and ESP32-S3-WROOM-1U Datasheet*, 2023. [Online]. Available: https://www.espressif.com/sites/default/files/documentation/esp32-s3-wroom-1_wroom-1u_datasheet_en.pdf.

[3] InvenSense, *MPU-6000 and MPU-6050 Product Specification, Revision 3.4*, 2013. [Online]. Available: https://invensense.tdk.com/wp-content/uploads/2015/02/MPU-6000-Datasheet1.pdf.

[4] Texas Instruments, *LM2596 SIMPLE SWITCHER Power Converter 150 kHz 3-A Step-Down Voltage Regulator*, 2020. [Online]. Available: https://www.ti.com/lit/ds/symlink/lm2596.pdf.

Appendix A Requirements and Verification Table

All verification procedures below were performed on the fully assembled robot unless otherwise noted. Quantitative results are summarized in Table 3 in Section 3.

Table 7: Full Requirements and Verification Table

Requirement	Verification Procedure	Result
Control Subsystem		
Bluetooth end-to-end latency ≤ 150 ms.	1. Establish Bluetooth connection between Xbox controller and robot. 2. Record controller input and robot motor response simultaneously using iPhone slow-motion camera (240 fps). 3. Count frames between stimulus and response; convert to milliseconds. 4. Repeat over 10 trials; report mean.	50 ms average. **Pass.**
Detect communication loss and initiate emergency shutdown within 2 s.	1. Establish wireless connection; command motors to moderate speed. 2. Power off controller abruptly. 3. Observe robot behavior; time from power-off to all motors stopping. 4. Repeat three times.	All motors stopped within 2 s in all trials. **Pass.**
Drive Subsystem		
Linear acceleration ≥ 1.5 m/s^2 from rest on flat surface.	1. Mark two points 1 m apart on a flat surface. 2. Command full forward throttle from rest; record with stopwatch. 3. Compute acceleration: $a = 2d/t^2$ for distance $d = 1$ m. 4. Repeat three times; report mean.	3.6 m/s^2 measured. **Pass.**

Table 7: Full Requirements and Verification Table (continued)

Requirement	**Verification Procedure**	**Result**
Robot drives in both upright and inverted orientations.	1. Place robot upright; command forward drive; confirm directional motion. 2. Flip robot to inverted orientation; command forward drive; confirm motion. 3. Verify steering response in both orientations (self-adapting control logic).	Confirmed in both orientations with self-adapting control logic. **Pass.**
Drive wheels extend beyond chassis height to ensure ground contact in both orientations.	1. Measure wheel diameter with calipers. 2. Measure chassis height (top plate to bottom plate) with calipers. 3. Compute clearance: $\Delta h = (d_{wheel} - h_{chassis})/2$. 4. Verify $\Delta h > 0$ mm.	$d_{wheel} = 50$ mm, $h_{chassis} = 46$ mm, $\Delta h = 2$ mm. **Pass.**
Weapon Subsystem		
Drum tip speed ≥ 100 mph within 10 s of full throttle. (Original: ≥ 150 mph; revised for safety—see Section 3.3.)	1. Secure robot in test fixture with drum free to rotate. 2. Affix neodymium magnet to drum outer surface. 3. Position Hall effect sensor ≈ 5 mm from magnet path. 4. Command full weapon throttle; record pulse period at $t = 10$ s. 5. Compute tip speed: $v = \pi d_{drum} \cdot f$.	112 mph (50.0 m/s) measured. Revised requirement met. **Pass.**
Power Subsystem		

Table 7: Full Requirements and Verification Table (continued)

Requirement	Verification Procedure	Result
Battery provides ≥ 2 minutes of continuous operation under typical combat loading.	1. Fully charge 3S battery to 12.6 V (4.2 V/cell). 2. Run robot through simulated 2-minute match: alternate drive and weapon engagement in representative duty cycle. 3. Monitor battery voltage via voltmeter at test end. 4. Verify voltage ≥ 9.9 V (3.3 V/cell) at 2-minute mark.	10.3V measured. **Pass.**
Structure Subsystem		
Total assembled weight < 907 g (2.0 lb) including battery.	1. Weigh fully assembled robot with battery installed on a digital scale. 2. Verify weight < 907 g.	640 g measured. **Pass.**
Stability & Recovery Subsystem		
Gyroscopic correction algorithm activates when IMU detects flip motion (pitch/roll rate > 5 rad/s).	1. Mount robot on a pivot allowing single-axis rotation. 2. Rotate at known angular rates (below and above 5 rad/s). 3. Log serial output from ESP32-S3 to confirm activation flag. 4. Verify: no activation below threshold; consistent activation above.	Not tested (deferred to future work). **N/A.**

Appendix B PCB Schematic and Layout

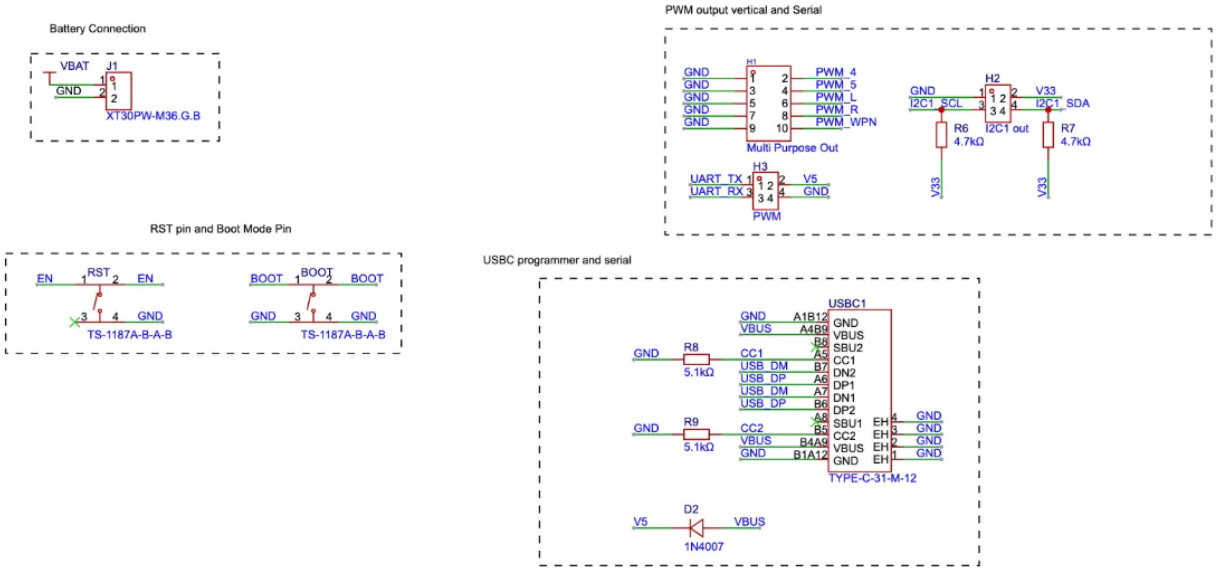

Figure 4: ESP32-S3 carrier PCB schematic, page 1 of 4.

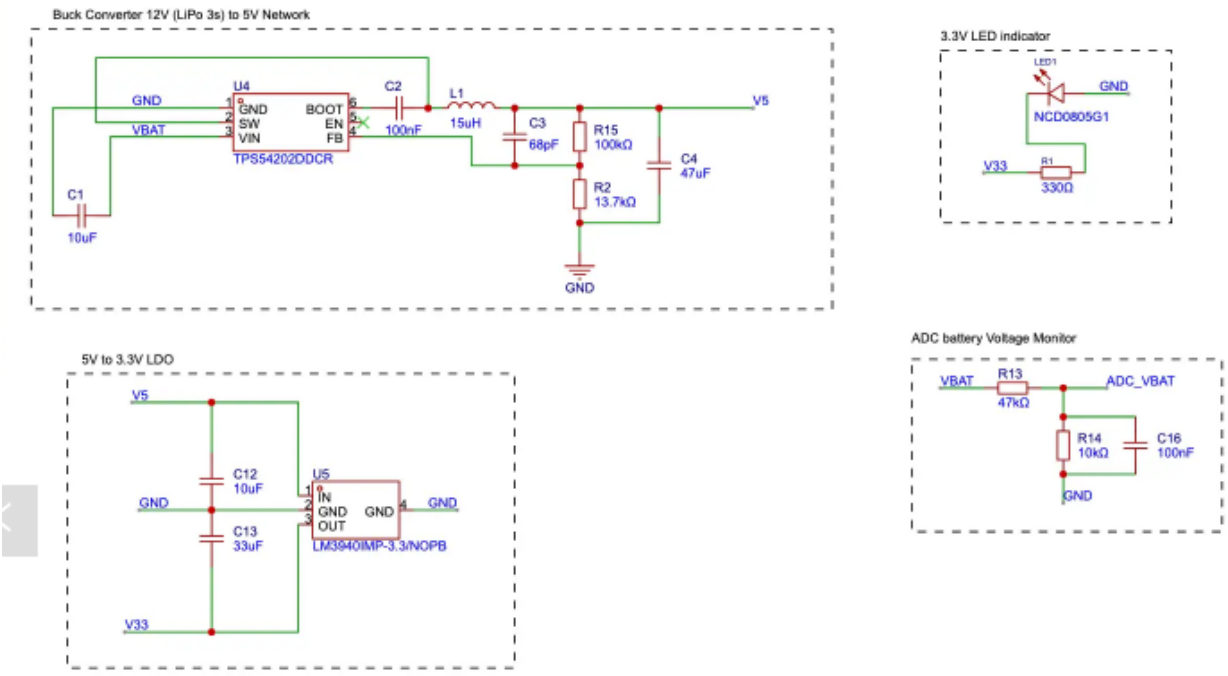

Figure 5: ESP32-S3 carrier PCB schematic, page 2 of 4.

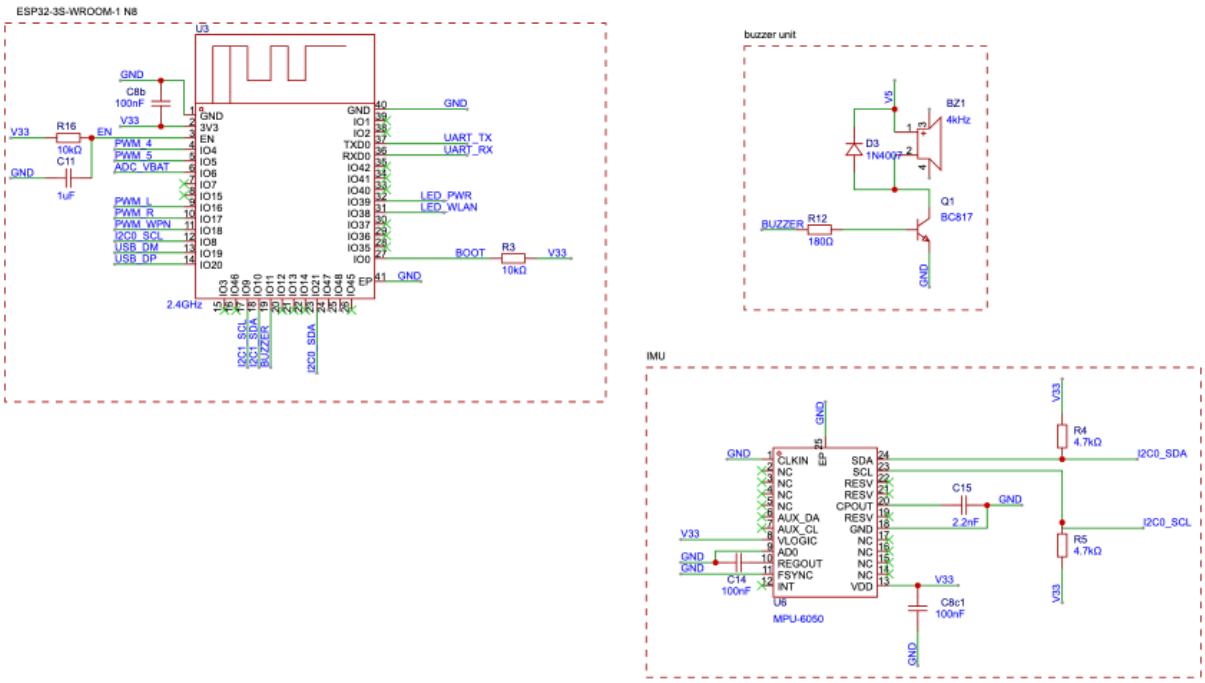

Figure 6: ESP32-S3 carrier PCB schematic, page 3 of 4.

Figure 7: ESP32-S3 carrier PCB schematic, page 4 of 4.

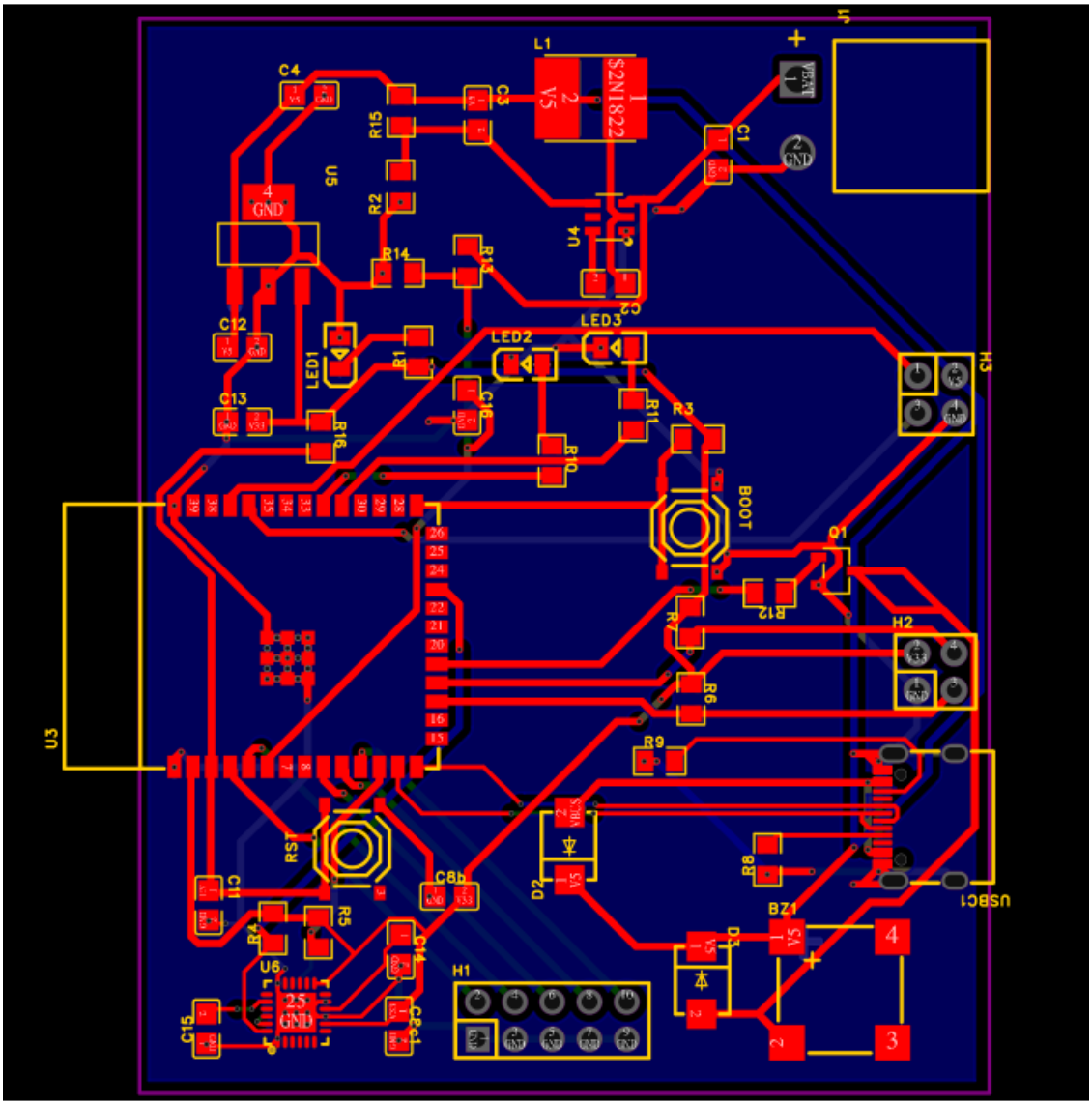

Figure 8: PCB layout showing component placement and copper routing.